

P1-14 Characteristics of Dual Wavelength 1064nm and 532nm Lidar Signals using Si-Avalanche Photodiode Single Photon-Counting Modules

Kenji TATSUMI and Tadashi IMAI

Office of Research & Development, National Space Development Agency of Japan,

2-1-1, Sengen, Tsukuba-shi, Ibaraki, 305-8505, JAPAN

TEL:+81-298-52-2275, FAX:+81-298-52-2299, E-mail:tatsumi.kenji@nasda.go.jp

1. Introduction

Lidar technologies have made remarkable advances lately. Within the past few years, laser diode pumped solid-state lasers have been developed for space application and avalanche photodiodes (APD's) have also become available^{1,2)} for single photon counting. When operated in the Geiger mode, they have detection efficiencies for single photons in the about 30% range for visible light and in the 1% range for the infrared light. The detection efficiency of the APD at the wavelength of about 1,000nm is higher than that of the conventional photomultiplier tubes. The high quantum efficiency of the silicon Geiger mode APD detectors is a major advantage for spaceborne lidar. These detectors are planned to be used for the ELISE³⁾ (Experimental Lidar In Space Equipment developed by NASDA), which is a Mie lidar to measure three dimensional distribution of clouds and aerosols, and for the GLAS⁴⁾ (Geoscience Laser Altimeter System, NASA).

The characteristics of 1064nm lidar signal using Si-APD single photon-counting module (SPCM) was previously described⁵⁾. In this paper we report the characteristics of dual wavelength 1064nm and 532nm lidar signals using Si-APD SPCM's.

2. Calculation of Signal to Noise Ratio

A received photo-electron data of lidar observation is M pieces of a time series data corresponding to each range bin in one measurement. If the N times measurements are repeated under the same condition, MxN data set is obtained.

A signal to noise ratio (S/N) may be defined as the ratio of the mean \bar{n}_j^s to the standard deviation σ_j of the number of detected photons at each gated time j corresponding to the range bin.

$$\begin{aligned} (S/N)_j &\equiv \bar{n}_j^s / \sigma_j \\ \bar{n}_j^s &= \frac{1}{N} \sum_{i=1}^N n_{ij}^s, \quad \bar{n}_j = \frac{1}{N} \sum_{i=1}^N n_{ij} \\ \sigma_j^2 &= \frac{1}{N} \sum_{i=1}^N (n_{ij} - \bar{n}_j)^2 = \bar{n}_j^2 - \bar{n}_j^2 \end{aligned} \quad (1)$$

The number of photons being counted in the gated time should be a Poisson random variable⁶⁾ with mean value equal to m . The Poisson probability density function is given by

$$P(x) = \frac{m^x e^{-m}}{x!} \quad (2)$$

where $x=0,1,2,\dots$ are random variable.

Variance σ_x^2 and standard deviation σ_x are given by

$$\sigma_x^2 = m, \quad \sigma_x = \sqrt{m} \quad (3)$$

In lidar measurement received light n_{ij} is comprised of signal n_{ij}^s scattered from cloud, aerosol and air molecule, background light n_{ij}^b , and dark-count n_{ij}^d

$$n_{ij} = n_{ij}^s + n_{ij}^b + n_{ij}^d \quad (4)$$

Thus variance σ_j^2 of the received photo-electron data is $\sigma_j^2 = \bar{n}_j$. The signal to noise ratio S/N is given by

$$S/N = \bar{n}_j^s / \sqrt{\bar{n}_j} \quad (5)$$

On the other hand, the numerator \bar{n}_j^s of the equation (5) is calculated by $\bar{n}_j^s = \bar{n}_j - \bar{n}_j^B$ using the relation of $\bar{n}_j = \bar{n}_j^s + \bar{n}_j^B$ and $\bar{n}_j^B = \bar{n}_j^b + \bar{n}_j^d$. If background noise and dark counts are independent of time and average values of each data are constant, \bar{n}_j^B is given by the average value of background and dark counts under the condition $n_{ij}^s \ll n_{ij}^B$. The S/N is calculated by

$$S/N = (\bar{n}_j - \bar{n}_j^B) / \sqrt{\bar{n}_j} \quad (6)$$

Considering the accumulation number, the S/N of the detected number of the photons is given by,

$$S/N = \sqrt{K} \cdot (\bar{n}_j - \bar{n}_j^B) / \sqrt{\bar{n}_j} \quad (7)$$

where K is accumulation number.

3. Experimental Setup

The schematic of the lidar is shown in Fig.1. The transmitter of the lidar consists of a laser diode pumped Q-switched Nd:YAG laser and KTP's second harmonic generator. The maximum output energy of Nd:YAG laser is 100mJ with the wavelength of 1064nm, the pulse width is 30ns, and the pulse repetition rate is 30pps. The output energies at the transmission optics are 20mJ for 1064nm and 5mJ for 532nm, respectively. Both beam divergence is 0.5mrad.

The receiver of the lidar is based on a 300-mm Cassegrain telescope. The aft optics includes a collimating lens before a filter and a focusing lens to image the primary mirror on the detector. The field of view is 0.7mrad. The band width of the interference filter inserted into the receiver is 2nm, which rejects the back ground noise. In order to secure a linearity of the photo-detector, the received light level was controlled by a neutral density (ND) filter whose transmittance is proofreaded.

The receiver employs a photon counting solid state Geiger mode avalanche photodiode module whose model number is SPCM-AQ-212 which was made by EG&G, Canada. The module consists of a Si-APD, discriminator, active quenching circuit, high voltage bias circuit, and thermal controller. In the Geiger mode, an APD is biased above its breakdown voltage for operation at very high gain. When biased above breakdown, the APD will normally conduct a large current. However, if this current is limited to less than the APD's latching current, there is a strong statistical probability that the current fluctuate to zero in the multiplication region, and the APD will then remain in the off state until an avalanche pulse is triggered by either a bulk or photo generated carrier. If the number of bulk carrier generated pulses is low, the APD can therefore be used to count individual current pulses from incident photons.

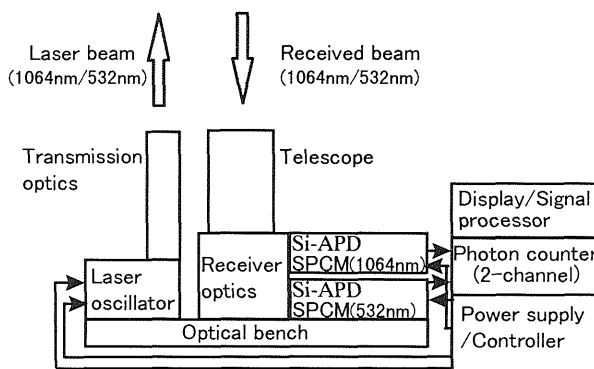


Fig. 1. The schematic of the lidar.

The outside diameter of the Si-APD is 0.5mm, but the effective diameter is 0.45mm. The measured detection probability is 1% at the wavelength of 1064nm and 33% at the wavelength of 532nm. The dark count rate is 500c/s for 1064nm and 890c/s for 532nm. The linearity correction factor is 1.10 @1Mc/s for each module.

The vertical resolution was 75m which corresponds to the gate time of 500ns.

The specifications of the lidar are summarized in Table 1.

4. Experimental Results

The experiments were accomplished from 17:15 to 19:05 JST at Nov.25,1998 in Tsukuba Space Center of NASDA. High atmospheric pressure covered Japan widely in that day. It was very fine day with moderate westerly winds, and there was not a speck of cloud in the sky and no aerosol in the vicinity of the surface. The lidar operated simultaneously at 1064nm and 532nm wavelength, and was zenith-pointing from a ground.

The measured data before and after experiment is shown in Fig.2. The data accumulation number is 10,000, and the measured S/N is about 33 at the altitude of 12km for the wave length of 1064nm. These data indicate that the atmospheric state was stable and not changed during the experiment. Thus, obtained data was regarded as observation data under the same conditions.

Because it was very clear in that day, we compared the experimental results with the simulation which the air molecular scattering was only considered. The calculated results were in good agreement with the experimental results.

Table 1 The specifications of the lidar.

Items	Specifications	
Trasmitter	Laser	LD pumped Q-switched Nd:YAG laser
	Wavelength	1064nm & 532nm
	Laser output energy	100mJ(Maximum)
	Transmitted energy	20mJ(1064nm), 5mJ(532nm)
	Pulse repetition rate	30pps
	Pulse width	30ns
	Beam divergence	0.5mrad
Receiver	Diameter of telescope	300mm ^φ
	Transmission	Variable using ND filter
	Field of view	0.7mrad
	Band width of filter	2nm
	Parallax	880mm
Detector	Detection method	Si-APD Single Photon Counting
	Model number	EG&G:SPCM-AQ-212
	Detection probability	1.0%@1064nm,33.0%@532nm
	Dark counts	500c/s@1064nm,890c/s@532nm
	Vertical resolution	75m(Gate time 500ns)

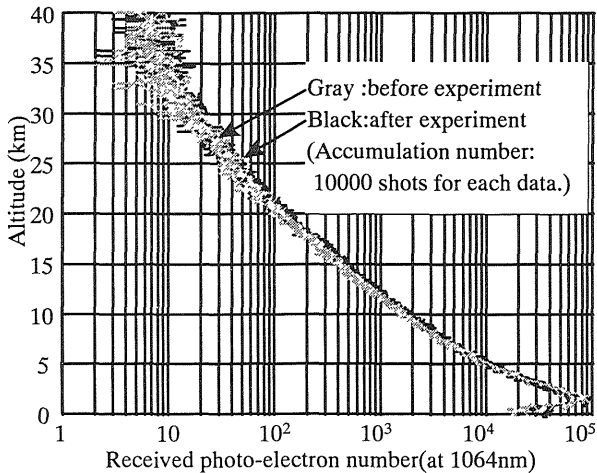
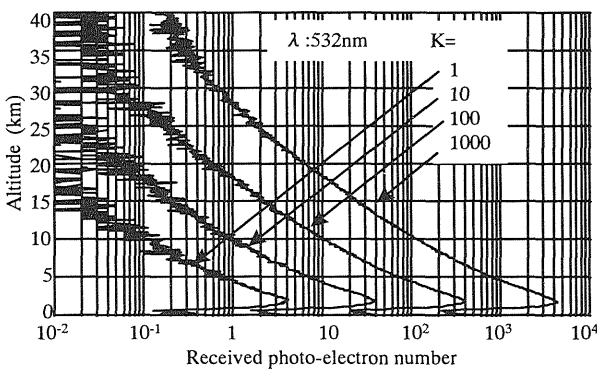


Fig.2. Received photo-electron number before and after experiments. Time is 17:15 JST before experiment and 19:05 after experiment.

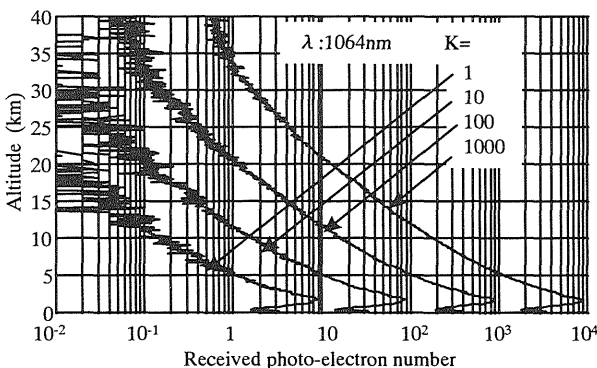
In order to evaluate S/N and a distribution function of received photo-electron, the accumulation number was changed as 1,10,100, and 1000 times. In each observation measurements were repeated 100 times over.

The relation between the received photo-electron number and the altitude as accumulation number changed is shown in Fig.3.

The received photo-electrons increase in proportion to accumulation number.



(a) In case of 532nm wavelength

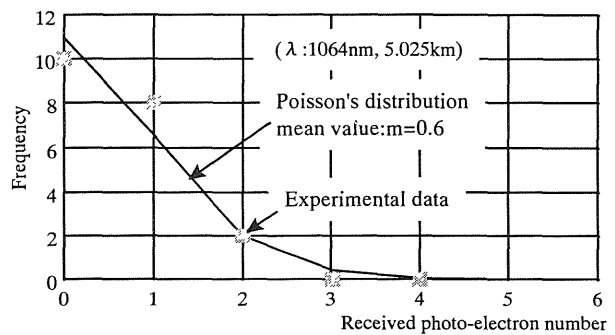


(b) In the case of 1064nm wavelength.

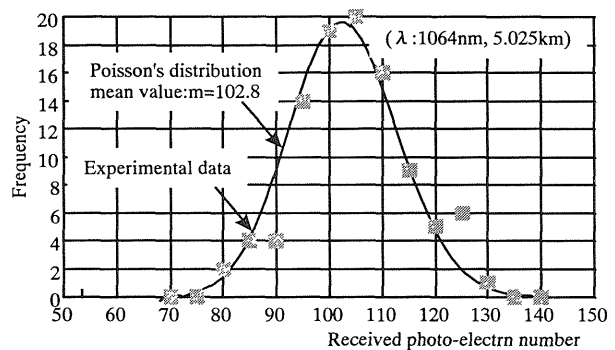
Fig.3. Received photo-electron number as accumulation number changed.

Figure 4 shows a distribution of the received photo-electrons with the wavelength of 1064nm. The accumulation number K of the measured value in Fig.4 (a) is unity and the altitude is 5.025km. In this figure, the solid line is the calculated value using Poisson's distribution function with the mean value of 0.6. The calculated value almost agrees with the measured value. Fig.4 (b) is in the case of the accumulation number of 100 at the altitude of 5.025km. In this case the distribution is Poisson's one with the mean value of 102.8. The distribution function is nearly Gaussian, because of the large input photo-electrons

The same characteristics of the received photo-electron distribution were also obtained in case of 532nm wavelength.



(a) In case of the accumulation number of 1.



(b) In case of the accumulation number of 100.

Fig.4. Received photo-electron distribution with the wavelength of 1064nm.

Figure 5 shows the relation between the mean value m / variance σ^2 and the altitude obtained from the measured values. In the figure, the black solid line is the data at the wavelength of 1064nm, the gray line is at 532nm. The ratio of mean value to variance is almost unity above the altitude of 2.5km. Thus the distribution of the received photo-electron is verified to be Poisson's distribution.

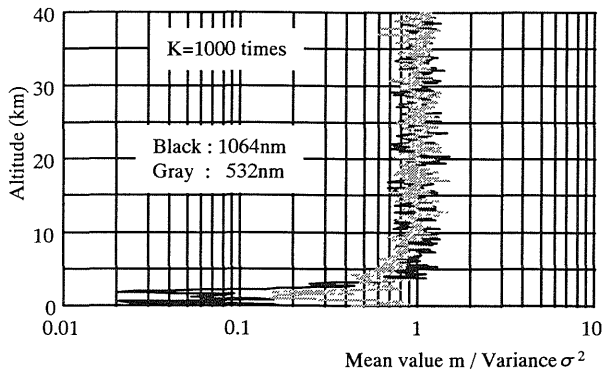
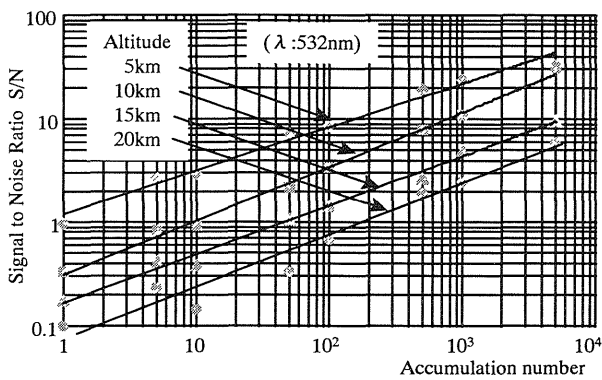
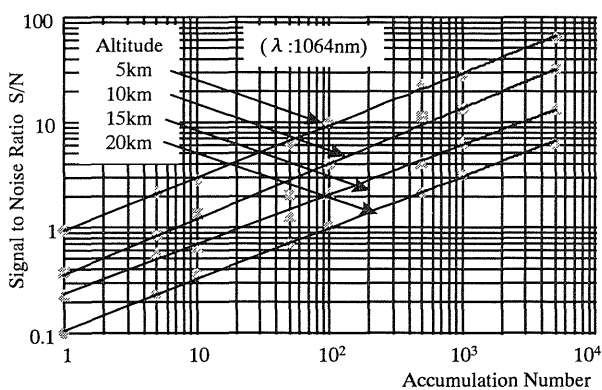


Fig.5. Relation of m/σ^2 vs. altitude. The data below the altitude of 2.5km is invalid because of parallax between transmitter optical axis and receiver optical axis.

The relation between the accumulation number and the signal to noise ratio S/N is shown in Fig.6. The parameter is the altitude. The solid lines in this figure are obtained from the results using a least squares method. The S/N is approximately proportion to the square root of the accumulation number.



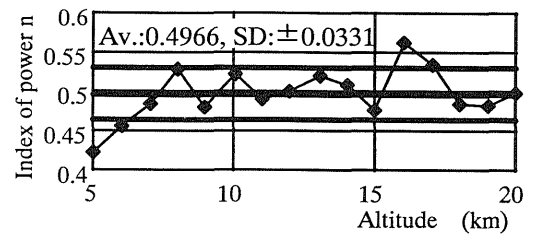
(a) In the case of the wavelength 532nm



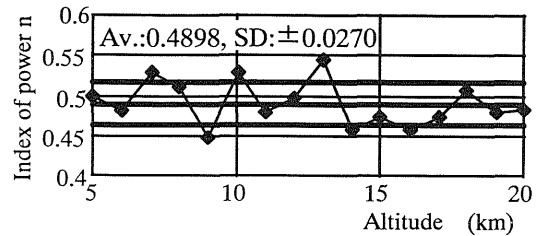
(b) In the case of the wavelength 1064nm

Fig.6. Relation of the accumulation number and signal to noise ratio. S/N increases in proportion to square root of accumulation number.

If the S/N be proportion to the n-th power of accumulation number K, we calculated the index of n from the measured values as the altitude changed. The results are shown in Fig.7. The averaged value and the standard deviation are 0.4966, 0.0331



(a) In the case of 532nm wavelength



(b) In the case of 1064nm wavelength

Fig.7. Index of power n

respectively in case of the wavelength of 532nm. In the case of 1064nm wavelength, the averaged value is 0.4898, and the standard deviation is 0.0270. These results verify that the S/N is proportion to the square root of the accumulation number for both cases.

5. Conclusions

We reported characteristics of the dual wavelength lidar signals using Si-APD single photon counting modules as photo-receiver. Experimental results show that the distribution of received photo-electron signal from the atmosphere is a near Poisson's distribution, and the signal to noise ratio increases exactly in proportion to the square root of accumulation number.

References

- 1)H.Dautet,P.Deschamps,B.Dion,A.D.MacGregor,D.MacSween, R.J.Mcintyre,C.Trottier,andP.P.Webb:Appl.Opt.**32**,(1993) 3894-3900.
- 2)X.Sun,andF.M.Davidson:J.ofLightwaveTech.**10**,(1992) 1023-1032.
- 3)K. Tatsumi, T. Imai, Y. Kawamura, N.Tanioka, T. Aoyagi, and T. Takada : Proc. of the 1st work shop on Mission Demonstration Satellite Lidar, Earth Science & Technology Organization (1998) 16-22
- 4)J.B.Abshine: Proceeding of 19th ILRC, Annapolis, Maryland July, (1998) 211-214
- 5)K.Tatsumi and T.Imai: The Review of Laser Eng. **27** (1999) 190-193.
- 6)E.Hanamura :*Quantum Optics*.(Iwanami Shoten, Publishers, 1992) p.72